Case study 001 - public WFC3/IR data

Diagnosing a hidden ramp transient in WFC3/IR HgCdTe data

Why spatial inspection alone would accept affected reads - and bias the final count-rate product.

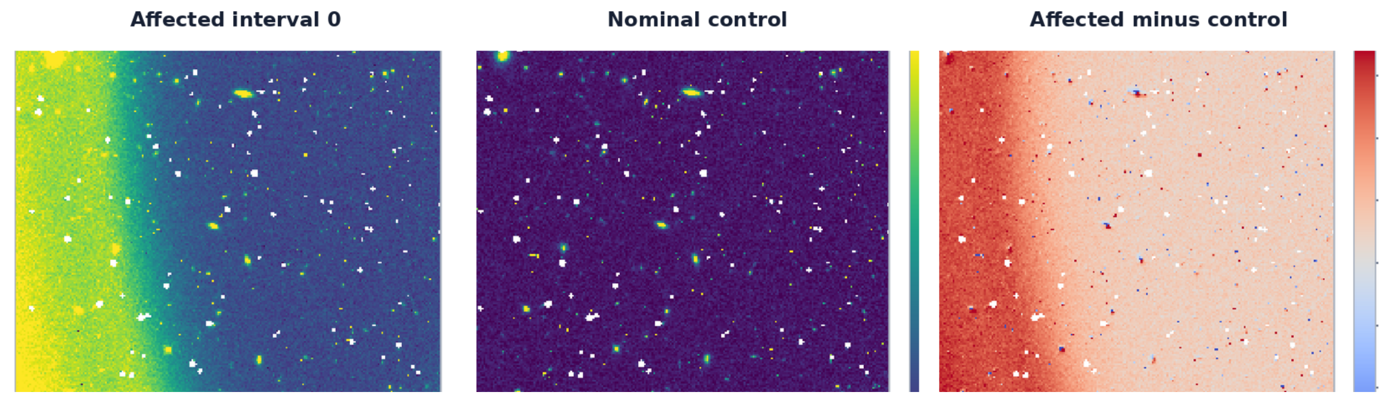

0 to 3
Spatially anomalous intervals

0 to 6
Common-mode intervals

700 s
Transient duration

16.1%
Excess relative to nominal charge

> The strong spatial gradient disappears while the control-relative transient persists. A spatial-only diagnostic would stop three intervals too early.

Analysis by Brooks Photonics using public HST WFC3/IR measurements from MAST.
No client data are represented.

BP-CS-001-C
Rev 1.7 · 2026-08-01

Finding and method

Read-level evidence identifies a time-variable external background

Intervals **0 to 3** contain pronounced left-right structure. A lower-amplitude detector-wide excess remains through interval **6**, producing a total transient duration of **700 s**. No intrinsic detector-material explanation is required by the data.

Supported mechanism: time-variable external background

The effect decays within one exposure, is absent from the matched control, survives source masking, and changes the reconstructed slope.

Reconstruct charge
Recover cumulative charge from calibrated reads.

Measure intervals
Calculate consecutive-read rates.

Separate modes
Evaluate spatial and common-mode behavior independently.

Refit the ramp
Exclude the transient and compare the result.

53.85%
Peak affected asymmetry
1.83% in the nominal control.

0.4958
Peak excess rate
electrons s^{-1} $pixel^{-1}$ after control and offset correction.

94.25%
Source-free pixels retained
Classification agreement remains 100%.

2,000
Bootstrap replicates
All retain the nominal 700 s duration.

Relevance to detector development and production

- Detect time-dependent artifacts hidden by final fitted outputs.
- Separate device nonuniformity from common-mode test conditions.
- Quantify decision sensitivity and uncertainty.
- Specify the minimum additional measurement needed to resolve ambiguity.

Source distinction. STScI documents the affected/control exposure pair, the Earth-limb scattered-light interpretation, and the read-level visualization example. Brooks Photonics independently adds spatial-versus-common-mode endpoint separation, source-mask and threshold sensitivity tests, block-bootstrap uncertainty, and quantitative post-transient refitting.

Spatial evolution

The gradient collapses first; the common-mode tail remains

Three decision-relevant stages show the transition from an obvious spatial anomaly to a temporally elevated but visually subtle detector state.

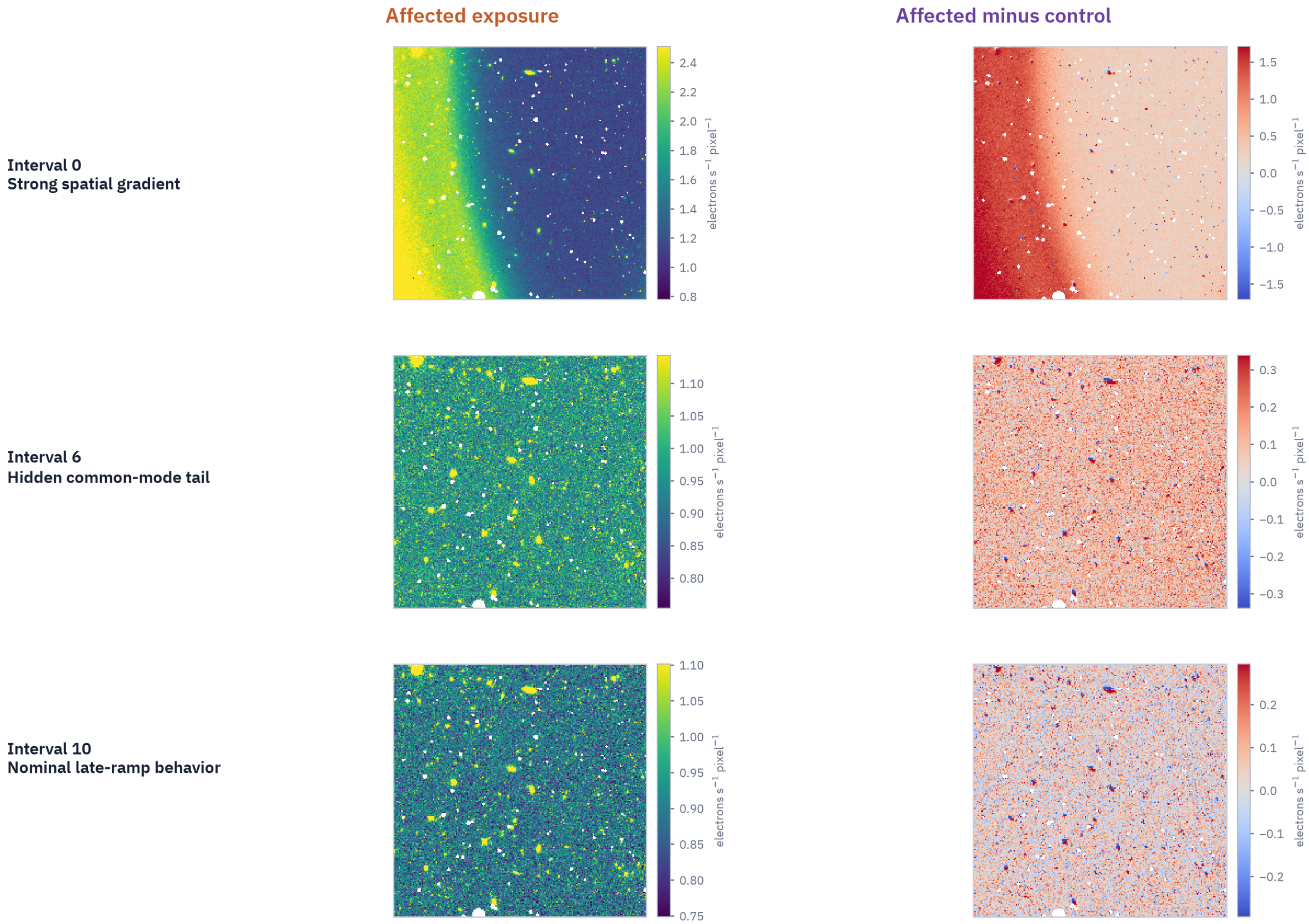

Figure 1. Affected exposure and affected-minus-control maps for intervals 0, 6, and 10. The map scales remain interval-specific to preserve spatial detail; quantitative acceptance is determined from the temporal analysis on the next page.

Temporal diagnosis and robustness

Three affected intervals remain after visual stabilization

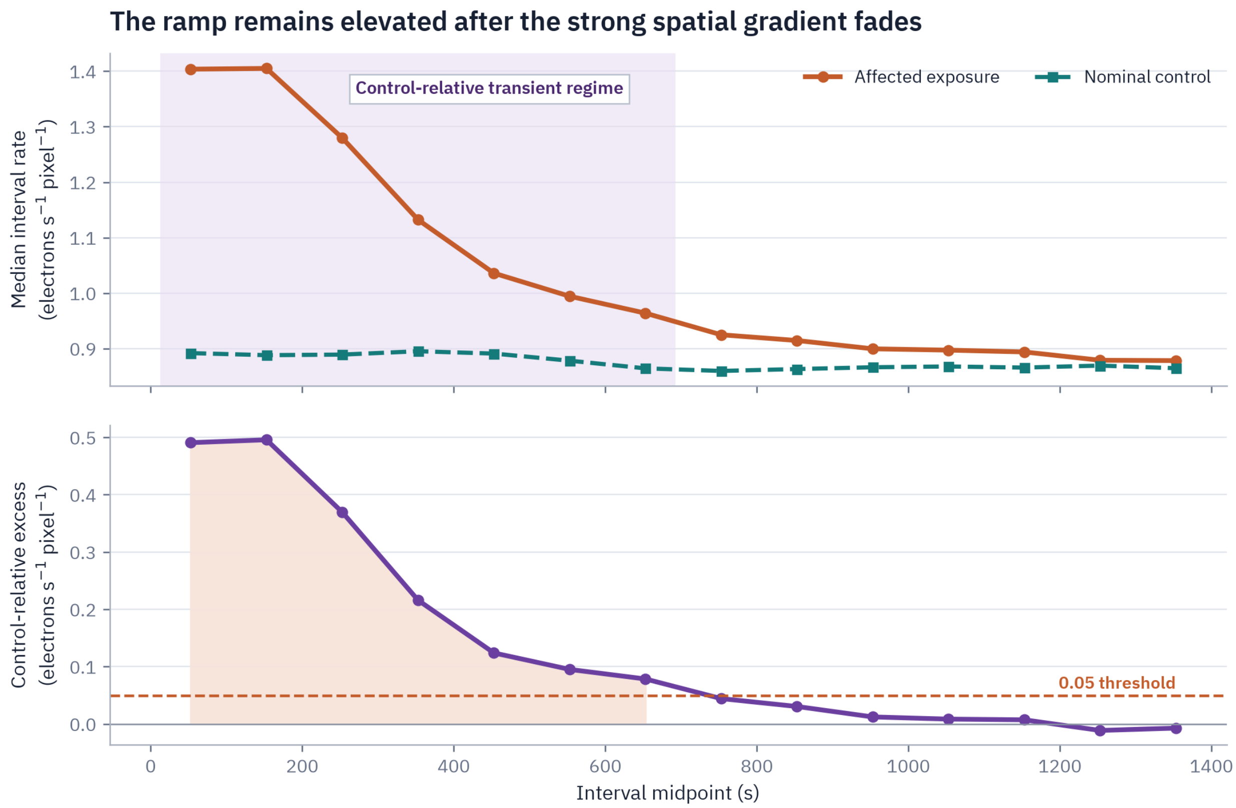

Figure 2. Intervals 0 to 6 exceed the nominal 0.05 electrons s^{-1} $pixel^{-1}$ limit after matched-control subtraction and late-offset removal. The limit is 4.28 times the robust late-ramp residual scale (0.01167 electrons s^{-1} $pixel^{-1}$) and is not an official WFC3 pipeline threshold.

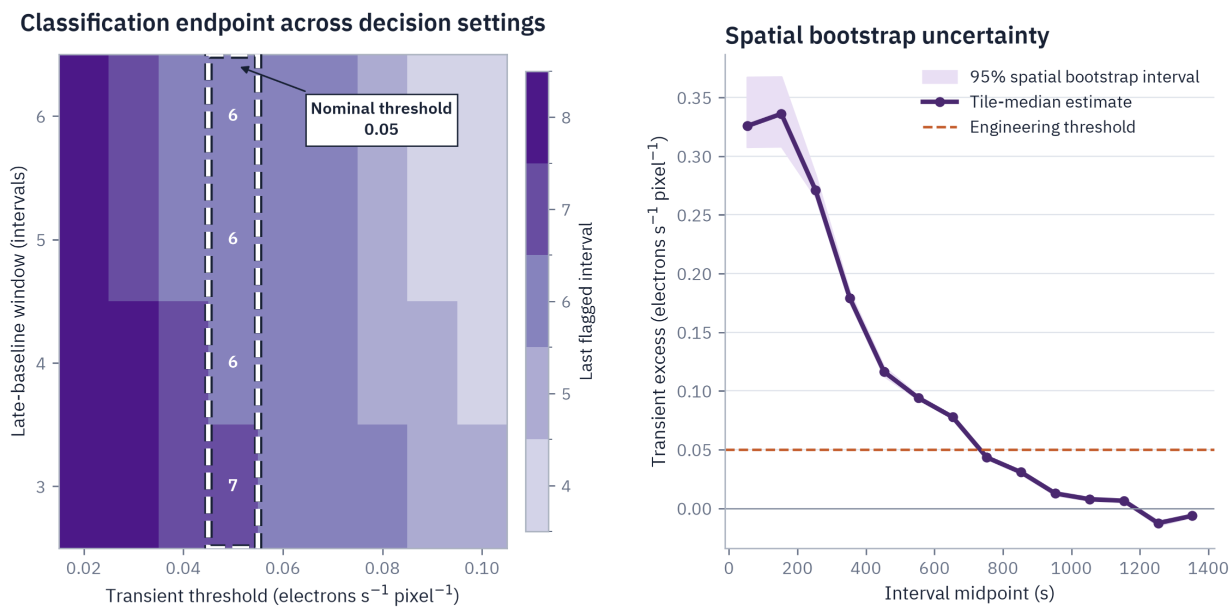

Figure 3. The decision endpoint is stable across threshold and late-baseline choices. Spatial block resampling preserves the 700 s classification duration.

Estimator distinction. The detector-wide median gives 197.26 electrons $pixel^{-1}$; the spatially robust tile-median gives 150.03 electrons $pixel^{-1}$. These are different estimands, not competing estimates of one quantity.

Independent reconstruction

Excluding the transient changes the inferred count-rate product

A free-intercept, DQ-aware ordinary-least-squares fit begins at **702.934 s**, after interval 6. Early excess charge is then absorbed by the intercept rather than forcing the later slope upward.

Archived and independently reconstructed count-rate products

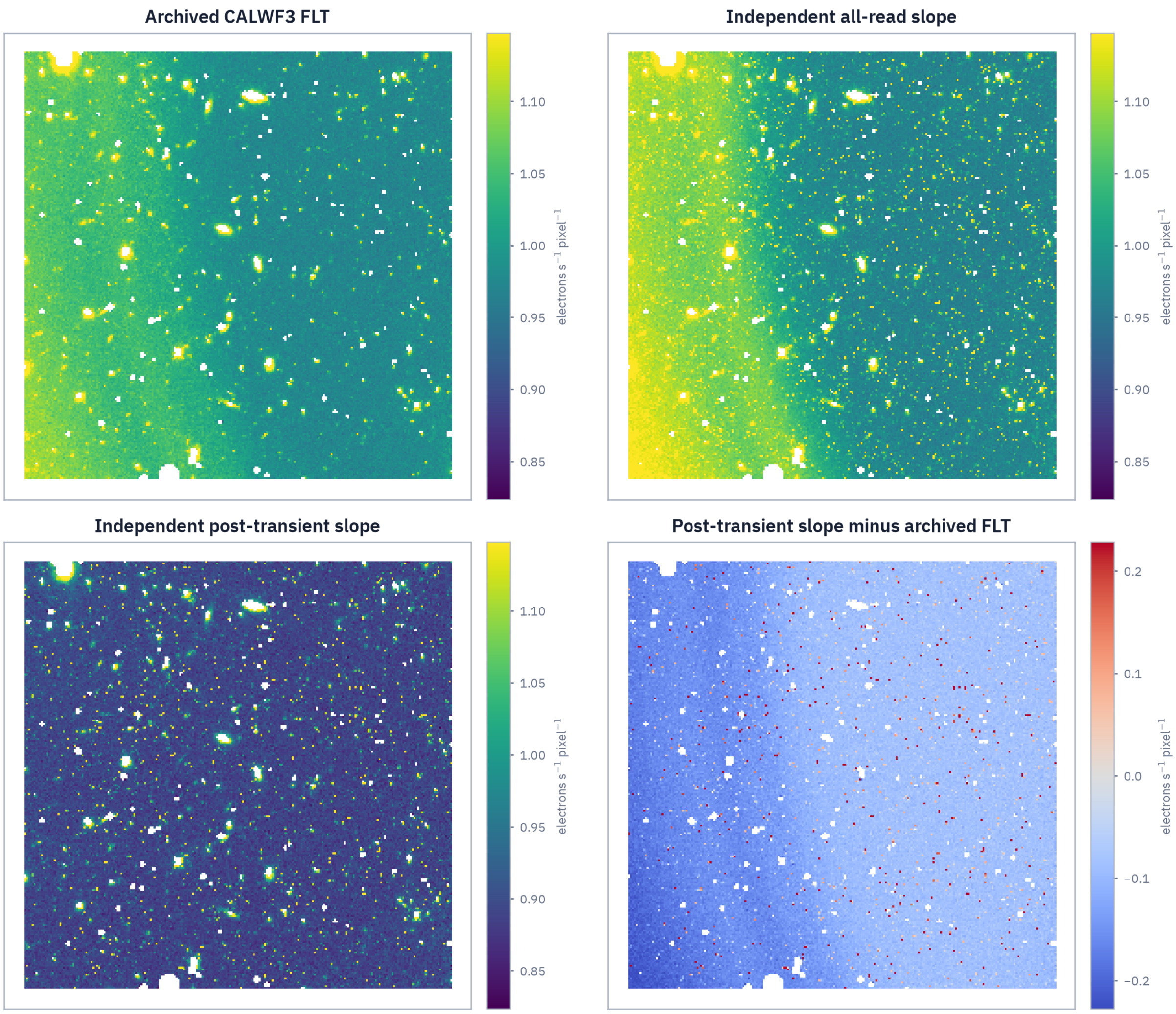

Figure 4. Archived CALWF3 FLT, independent all-read slope, independent post-transient slope, and post-transient-minus-FLT residual.

6.32% to 0.40%
Left-right asymmetry after transient exclusion

0.11108
Lower than archived FLT in electrons s^{-1} pixel^{-1}

PRODUCT OR FIT	SOURCE-FREE MEDIAN	LEFT-RIGHT ASYMMETRY
Archived CALWF3 FLT	1.00296 electrons s^{-1} pixel^{-1}	6.32%
Independent all-read fit	0.99992 electrons s^{-1} pixel^{-1}	9.55%
Independent post-transient fit	0.89337 electrons s^{-1} pixel^{-1}	0.40%

Engineering disposition

Test temporal and spatial integrity separately

1. **Inspect consecutive-read maps**
   Do not accept a final slope product without interval-level review.
2. **Classify spatial and common-mode effects independently**
   A detector can appear uniform while retaining a measurable temporal background.
3. **Use a matched control or validated late baseline**
   Separate static offsets from decaying transients before thresholding.
4. **Quantify decision sensitivity**
   Report threshold, baseline, source-mask, and spatial-resampling dependence.
5. **Refit after transient exclusion**
   Compare slope, residual structure, and operational metrics with the production result.

Evidence-rating standard

Supported	Consistent with all principal observations.
Plausible secondary	May contribute, but cannot explain the full result.
Disfavored	Conflicts with one or more major observations.
Not evaluated	Insufficient evidence in the available data.

MECHANISM	ASSESSMENT
Time-variable external background	**Supported** Temporal decay, spatial evolution, and control comparison agree.
Readout-quadrant offset	**Plausible secondary** May contribute, but cannot explain the smooth detector-wide decay.
Stable gain or flat-field nonuniformity	**Disfavored** Expected to persist and appear similarly in the control.
Intrinsic dark-current nonuniformity	**Disfavored** The pattern decays within one exposure.
Isolated cosmic-ray event	**Disfavored** Cannot explain detector-wide smooth decay.

Data provenance

Four pinned MAST products are verified by byte count and SHA-256. Raw FITS files remain outside Git; the repository stores exact URIs, derived tables, figures, tests, and the complete execution workflow. Open the repository and reproducibility package.

Primary references

[1] O'Connor, A., Khandrika, H., Mack, J., and Calamida, A. (2023), *WFC3/IR IMA Visualization Tools with an Example of Time Variable Background*, HST/WFC3 Notebooks, updated 2023-05-05.

[2] Pagul, A., Rivera, I., et al. (2024), *WFC3 Data Handbook*, Version 6.0, Space Telescope Science Institute.

[3] Mikulski Archive for Space Telescopes (MAST), HST public product archive and download API; products retrieved for Case 001 in 2026.

Interpretation boundary. This case does not infer HgCdTe composition, carrier lifetime, dark-current mechanism, responsivity, detectivity, or intrinsic material quality. The 0.05 electrons s^{-1} pixel^{-1} threshold was selected before the sensitivity sweep at 4.28 times the robust late-ramp residual scale (0.01167 electrons s^{-1} pixel^{-1}). It is a transparent engineering operating limit, not an official WFC3 pipeline threshold.